Polym. Bull. (2012) 68:1483–1500
DOI 10.1007/s00289-011-0696-4

ORIGINAL PAPER

Adsorption of [meso-tetrakis(4-sulfonatophenyl)porphyrinato]oxovanadate(IV)(4–) onto chitosan in aqueous solution

Tapan Kumar Saha · Md. Farhad Mahmud · Subarna Karmaker · Tusher Sen

Received: 28 August 2011 / Revised: 24 November 2011 / Accepted: 25 December 2011 /
Published online: 11 January 2012

Abstract Adsorption of [meso-tetrakis(4-sulfonatophenyl)porphyrinato]oxovanadate(IV)(4–), [VO(tpps)], onto chitosan 7B in aqueous solution was investigated in a batch system. The effects of solution pH, initial concentration of [VO(tpps)], and temperature were studied. Adsorption kinetic data obtained from different batch experiments was modeled using both pseudo first- and second-order kinetic equations. Freundlich, Tempkin, and Langmuir models were used for the description of adsorption equilibrium data. The best results were achieved with the pseudo second-order kinetic and Langmuir isotherm equilibrium models, respectively. The equilibrium adsorption capacity (q_e) increased with increasing the initial concentration of [VO(tpps)], showing maximum adsorption capacity of 441.21 μmol/g. The activation energy (E_a) of sorption kinetics was estimated to be 19.84 kJ/mol in the temperature range 25–40 °C. Thermodynamic parameters such as changes in free energy (ΔG), enthalpy (ΔH), and entropy (ΔS) were also evaluated by applying the Van't Hoff equation. The values of thermodynamic parameters of [VO(tpps)] adsorption onto chitosan 7B indicate its spontaneous and endothermic nature. The present work provides a first example for the preparation of chitosan–[VO(tpps)] complex in aqueous solution.

Keywords Chitosan · Oxovanadium(IV) porphyrin · Adsorption · Kinetics · Equilibrium

Introduction

Naturally occurring biopolymers have attracted considerable interest from polymer researchers in recent year [1–3]. This interest arose as a result of an increased

T. K. Saha (✉) · Md. F. Mahmud · S. Karmaker · T. Sen
Department of Chemistry, Jahangirnagar University, Savar, Dhaka 1342, Bangladesh
e-mail: tksaha_ju@yahoo.com

awareness of the environment and a desire to produce environmentally safe materials. Chitin is one of the most abundant and cheap forms of biomass, as well as cellulose. It is a main component existing in the shells of crustaceans, such as crabs, shrimps, prawns, insects, and centipedes, and is easily prepared from their shells at cheap cost by removing other components, calcium and proteins, by treating with acids and alkalis, respectively. Consequently, chitosan (Fig. 1a) is easily prepared from chitin by deacetylating its acetoamide groups with a strong alkaline solution. The high proportions of amino functions in chitosan have been found to provide novel adsorption properties for many metal ions [4] and organic dyes [5–11]. As a drug carrier, chitosan has also been widely used in the preparation of various biomedical products and their therapeutic activities have also been evaluated [12–14].

However, kinetics and binding constant of chitosan–drug complex, and its medicinal activity have not yet been studied extensively. Recently, we found that water soluble [meso-tetrakis(4-sulfonatophenyl)porphyrinato]oxovanadate(IV)(4–), [VO(tpps)] (Fig. 1b) in which the equatorial coordination sphere of vanadium is $VO(N_4)$, is a potential insulin-mimetic oxovanadium(IV)–porphyrin complex for the treatment of not only streptozotocin (STZ)-induced diabetic mice—a type 1 diabetic model—but also type 2 diabetic KKA^y mice when introduced by oral gavage [15, 16].

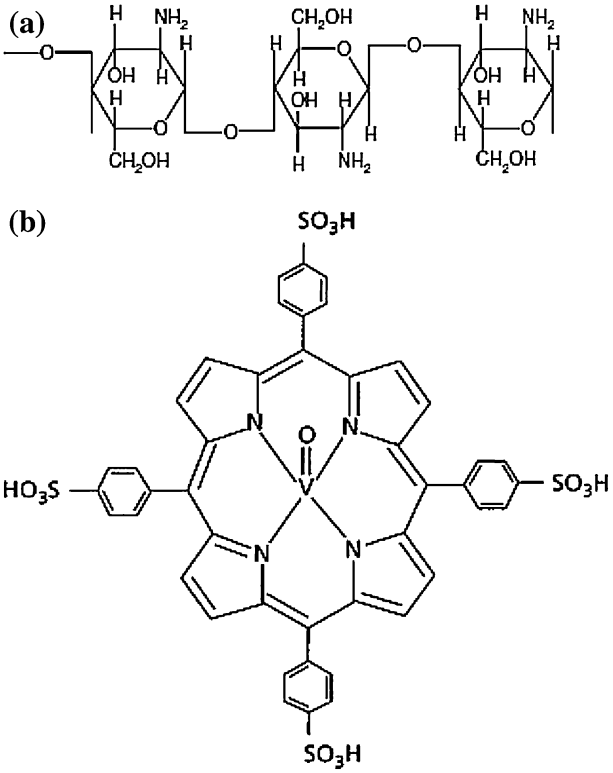

Fig. 1 The structures of chitosan 7B (**a**) and [VO(tpps)] (**b**)

The objective of this work was to explore the possible use of chitosan 7B (70% deacetylated) as a biodegradable adsorbent for the preparation of chitosan–[VO(tpps)] complex. [VO(tpps)] as shown in Fig. 1b is selected as a model of an anionic water soluble drug. The deacetylated amino groups in chitosan can be protonated and the polycationic properties of the polymer are expected to contribute to the charged interactions with [VO(tpps)]. The adsorption characteristics of [VO(tpps)] in aqueous solution onto chitosan were carried out through a series of batch adsorption experiments. The attention has been placed in an understanding of the kinetics; mechanisms, and equilibrium processes involved in adsorption of [VO(tpps)] onto chitosan 7B. Treatment of the chitosan surface with a cross-linking agent was not utilized in this study since cross-linking may change the properties of chitosan. The effects of pH, initial concentration of [VO(tpps)], and temperatures on the adsorption phenomena have been studied.

Experimental

Materials

All reagents and solvents were commercially available and of the highest grade of purity; hence, they were used without purification. Oxovanadium(IV) sulfate, $VOSO_4 \cdot nH_2O$, was obtained from Wako Pure Chemical Industries (Osaka, Japan). The ligand meso-tetrakis(4-sulfonatophenyl)porphyrin, H_2tpps, was purchased from Frontier Scientific Inc. (P.O. Box 31, Logan, UT, USA). $VOSO_4 \cdot nH_2O$ was standardized complexometrically with ethylenediamine-*N*,*N*,*N*′,*N*′-tetraacetic acid (EDTA), determined to be the trihydrate, and used in all of the experiments. Sephadex LH-20 was obtained from Amersham Pharmacia Biotech (Tokyo, Japan). [VO(tpps)] was synthesized and characterized as described previously [15].

Chitosan 7B (70% deacetylated) was obtained from Katokichi Bio Co., Ltd., Japan. The mass median diameters of the chitosan flakes were estimated to be (228 ± 5) μm using a laser scattering particle size analyzer (LDSA-2400A, Tonichi Computer Applications, Japan) equipped with a dry dispersing apparatus (PD-10S, Tonichi Computer Applications, Japan). Deionized water was prepared by passing distilled water through a deionizing column (Barnstead, Syboron Corporation, Boston, USA).

Batch adsorption experiments

The adsorption of [VO(tpps)] onto chitosan 7B was carried out in a 122 mL stoppered bottle at a constant room temperature (30 ± 0.2 °C) using a shaking thermostat machine at a speed of 120 r/min. The effect of pH on the adsorption of [VO(tpps)] onto chitosan 7B was examined by mixing 0.03 g of chitosan 7B with 25 mL of [VO(tpps)] (3 μmol/L) solution with the pH ranging from 5.0 to 9.0. The pH of the samples was adjusted either by adding microliter quantities of 1 mol/L HCl or 1 mol/L NaOH. In kinetics studies, 0.03 g of chitosan 7B was mixed with 25 mL of [VO(tpps)] solution with varied initial concentrations (2–10 μmol/L), and samples were withdrawn at desired time intervals. In equilibrium adsorption

experiments, 0.03 g of chitosan 7B was added to 25 mL of [VO(tpps)] solution with varied initial concentrations (1–1,000 μmol/L).

After equilibrium, the samples were centrifuged using a centrifuge machine (Labofuge 200, D-37520 Osterods, Germany) at a speed of 4000 r/min for 5 min. The concentrations of [VO(tpps)] in the supernatant liquor were determined by using standard curve. The absorbance of [VO(tpps)] in aqueous solutions was measured with a Shimadzu UV-1601PC spectrophotometer at 436 nm, equipped with an electronically thermostatic cell holder (Shimadzu); the quartz cell had a path length of 1.0 cm. Before each measurement, the base line of spectrophotometer was calibrated against solvent. The λ_{max} of [VO(tpps)] was found to be 436 nm at the pH ranging from 5.0 to 9.0. The standard curve was obtained by plotting absorbance versus concentration of [VO(tpps)].

The amount of adsorbed [VO(tpps)] onto chitosan at time t, q_t (μmol/g) was determined by

$$q_t = V(C_0 - C_t)/m \quad (1)$$

where C_0 (μmol/L) and C_t (μmol/L) are the liquid-phase concentrations of [VO(tpps)] at initial and any time t, respectively; V (L) is the volume of the [VO(tpps)] solution; and m (g) is the amount of dry chitosan 7B used.

The amount of adsorbed [VO(tpps)] onto chitosan at equilibrium time t, q_e (μmol/g) was determined by

$$q_e = V(C_0 - C_e)/m \quad (2)$$

where C_0 (μmol/L) and C_e (μmol/L) are the liquid-phase concentrations of [VO(tpps)] at initial and equilibrium time t, respectively; V (L) is the volume of the [VO(tpps)] solution and m (g) is the amount of dry chitosan 7B used.

The adsorption kinetics and equilibrium adsorption of [VO(tpps)] onto chitosan 7B were also performed at temperatures 25, 35, and 40 °C, respectively. The amount of adsorbed [VO(tpps)] with per gram chitosan 7B was determined in the same way as described above.

Results and discussion

Adsorption kinetics of [VO(tpps)] onto chitosan 7B

Effect of pH

Adsorption experiments were conducted with the pH ranging from 5.0 to 9.0 to avoid solubilization of chitosan in aqueous solution at very low pH [8]. The effect of pH on the kinetics of [VO(tpps)] adsorption by chitosan at 30 °C is shown in Fig. 2a, where the initial concentration of [VO(tpps)] was 3 μmol/L. The rate of uptake of [VO(tpps)] on the adsorbent material indicated that about 50 min was taken to reach the equilibrium time for all pHs. However, the data was taken for 80 min to make sure that full equilibrium was established. Before the equilibrium time, it indicates that the initial rate of adsorption (dq/dt) increases significantly with

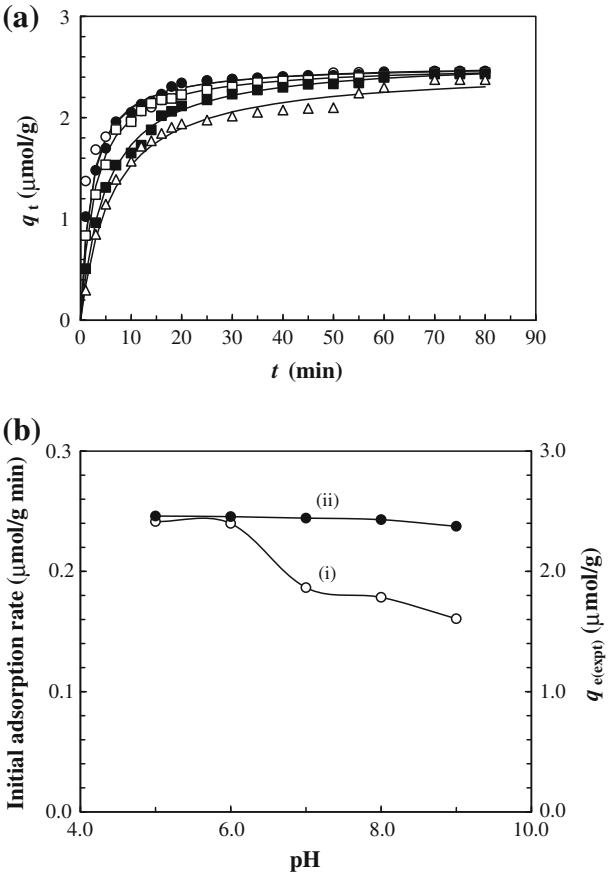

Fig. 2 **a** Adsorption kinetics of [VO(tpps)] onto chitosan 7B at different pHs (initial concentration of [VO(tpps)]: 3 μmol/L, solution volume 25 mL, chitosan 0.03 g, temperature: 30 °C, solution pHs: *opened circles* pH 5.0, *closed circles* pH 6.0, *opened squares* pH 7.0, *closed squares* pH 8.0, *opened triangles* pH 9.0). All *solid lines* are simulated adsorption kinetics of [VO(tpps)] onto chitosan at respective pHs. The simulated adsorption kinetic profiles were generated using the pseudo second-order model in Eq. 4 and the values of equilibrium adsorption capacity ($q_{e(cal)}$) and the pseudo second-order rate constant (k_2) listed in Table 1. **b** The changes of (*i*) initial adsorption rate (dq/dt) and (*ii*) equilibrium adsorption capacity ($q_{e(exp)}$) with pH. Data was taken from (**a**)

decreasing solution pH (Fig. 2b(i)). It can be seen that the pH of aqueous solution plays an important role on the rate of [VO(tpps)] adsorption onto chitosan. However, after 80 min of adsorption, the equilibrium adsorption capacity (q_e) was found to be 2.46–2.38 μmol/g at pH 5.0–9.0 (Fig. 2b(ii)). These results suggest that the initial solution pH does not affect the equilibrium adsorption capacity. Similar result was also observed in case of adsorption of H_2tpps onto chitosan 7B (data not shown). It may be caused by the gradual increase in initial pH of the reaction mixture during the progress of adsorption, and thus the final pH remained constant when the adsorption process reached at equilibrium (figure not shown). However, Yoshida et al. [5] and Kumar [6] reported that at lower pH more protons will be

available to protonate amino groups of chitosan molecules to form $-NH_3^+$ groups, thereby increasing the electrostatic attraction between negatively charged dye anions and positively charged adsorption sites and causing an increase in dye adsorption. This explanation does not agree well with our present results.

Effect of initial [VO(tpps)] concentration

The effect of initial concentration of [VO(tpps)] on the adsorption kinetics of chitosan 7B at pH 6.0 and temperature 30 °C is shown in Fig. 3a. An increase in the initial [VO(tpps)] concentration (2–10 μmol/L) leads to an increase in initial raising of adsorption rate (dq/dt) of [VO(tpps)] onto chitosan 7B. This is due to the increase in the driving force of the concentration gradient, as an increase in the initial [VO(tpps)] concentration. Similar results were obtained from the adsorption of methyl orange (MO) and reactive black 5 (RB5) in aqueous solution onto chitosan [10, 11], reactive red 189 (RR189) onto cross-linked chitosan beads [7] and reactive blue 19 (RB19) onto cross-linked chitosan/oil palm ash composite beads [9], respectively. It can also be seen from Fig. 3a that the equilibrium adsorption was achieved within 30–40 min in most of the cases. However, the data were taken for 80 min to make sure that full equilibrium was attained. Figure 3b shows the influence of initial [VO(tpps)] concentration on the equilibrium adsorption capacity (q_e) of chitosan 7B. It is clear that initial [VO(tpps)] concentration is an important factor affecting adsorption capacity of chitosan 7B. As shown in Fig. 3b, the equilibrium adsorption capacity of the chitosan 7B sharply increased from 1.52 to 367.82 μmol/g with increasing [VO(tpps)] concentration from 2 to 500 μmol/L, and tended to reach a weak saturation with further increasing [VO(tpps)] concentration. Chitosan flakes exhibit a maximum capacity 441.21 μmol/g.

Effect of temperature

The effect of temperature on the adsorption kinetics of [VO(tpps)] onto chitosan 7B at pH 6.0 is shown in Fig. 4 where the initial concentration of [VO(tpps)] was 3 μmol/L. Below and above the equilibrium time, an increase in the temperature leads to a slight increase in [VO(tpps)] adsorption rate (dq/dt) and adsorption capacity (q_t), which indicates a kinetically controlling process [7]. It can also be seen from Table 1 that the effects of temperature on the values of q_e are very insignificant as observed in the cases of adsorption of MO and RB5 onto chitosan 10B [10, 11]. It was also reported that the variation of solution temperature does not significantly affect the overall decolorization performance [6].

Rate constant studies

In order to investigate the mechanism of adsorption kinetics, the pseudo first-order and pseudo second-order equations were used to test the experimental data of pH, initial concentration, and temperature, respectively. Lagergren [17] expressed the pseudo first-order rate expression for the liquid–solid adsorption system and the most popular linear form is expressed as follows:

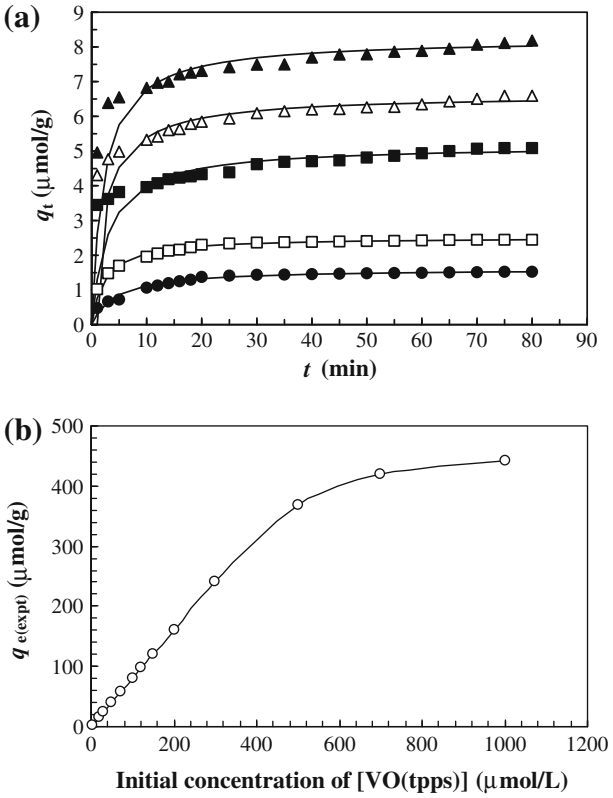

Fig. 3 **a** Adsorption kinetics of [VO(tpps)] on chitosan 7B at different initial concentrations. (solution volume 25 mL, chitosan 0.03 g, solution pH 6.0, temperature 30 °C, initial concentrations of [VO(tpps)]: *closed circles* 2 μmol/L, *opened squares* 3 μmol/L, *closed squares* 6 μmol/L, *opened triangles* 8 μmol/L, *closed triangles* 10 μmol/L). All *solid lines* are simulated adsorption kinetics of [VO(tpps)] onto the chitosan at respective initial concentrations of [VO(tpps)]. The simulated adsorption kinetic profiles were generated using the pseudo second-order model in Eq. 4 and the values of equilibrium adsorption capacity ($q_{e(cal)}$) and the pseudo second-order rate constant (k_2) listed in Table 1. **b** Effect of the initial [VO(tpps)] concentration on the equilibrium adsorption capacities of chitosan 7B (initial concentration of [VO(tpps)]: 2–1,000 μmol/L; solution volume: 25 mL; chitosan 7B: 0.03 g; solution pH: 6.0; temperature: 30 °C; equilibrium time: 80 min)

$$\log(q_e - q_t) = \log q_e - (k_1/2.303)t \tag{3}$$

where q_e (μmol/g) and q_t (μmol/g) are the amounts of [VO(tpps)] adsorbed onto chitosan at equilibrium and at any time t, respectively, and k_1 (1/min) is the rate constant of pseudo first-order adsorption. A straight line of $\log(q_e - q_t)$ versus t suggests the applicability of this kinetic model to fit the experimental data. The equilibrium adsorption capacity (q_e) is required to fit the data, but in many cases q_e remains unknown due to slow adsorption processes. Also, in many cases, the pseudo first-order equation does not fit well to the whole range of contact time and is generally applicable over the initial stage of the adsorption processes [17, 18].

The pseudo second-order kinetic model is expressed as [18, 19]:

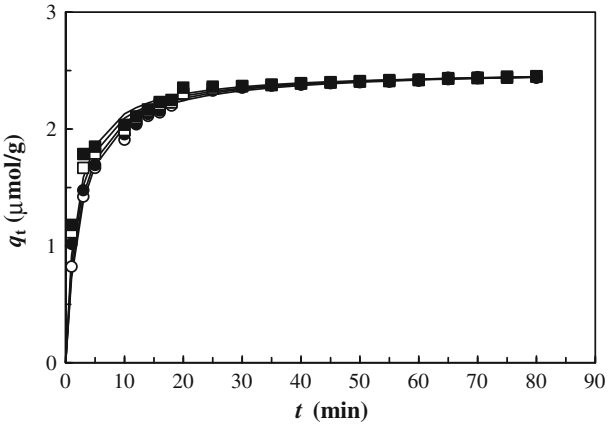

Fig. 4 Adsorption kinetics of [VO(tpps)] on chitosan 7B at different temperatures (initial concentration of [VO(tpps)]: 3 μmol/L, solution volume 25 mL, chitosan 0.03 g, solution pH 6.0, temperatures: *opened circles* 25 °C, *closed circles* 30 °C, *opened squares* 35 °C, *closed squares* 40 °C). All *solid lines* are simulated adsorption kinetics of VO(tpps)] onto the chitosan at respective temperature. The simulated adsorption kinetic profiles were generated using the pseudo second-order model in Eq. 4 and the values of equilibrium adsorption capacity ($q_{e(cal)}$) and the pseudo second-order rate constant (k_2) listed in Table 1

Table 1 Comparison of the pseudo first- and second-order rate constants, and calculated and experimental q_e values at various pHs, initial concentrations of [VO(tpps)], and temperatures

Parameters	$q_{e(exp)}$ (μmol/g)	First-order kinetic model			Second-order kinetic model		
		k_1 (1/min) (μmol/g)	$q_{e(cal)}$ (μmol/g)	R^2 (μmol/g)	k_2 (g/μmol min) (μmol/g)	$q_{e(cal)}$ (μmol/g)	R^2 (μmol/g)
pH							
5	2.46	0.0781	1.03	0.986	0.1892	2.53	0.999
6	2.46	0.0668	1.26	0.932	0.2006	2.52	0.999
7	2.44	0.0578	1.10	0.937	0.1458	2.52	0.999
8	2.43	0.0580	1.35	0.957	0.0789	2.58	0.999
9	2.38	0.0424	1.32	0.895	0.0650	2.48	0.996
Initial [VO(tpps)] concentration (μmol/L) (pH 6)							
2	1.52	0.0585	1.32	0.961	0.1452	1.61	0.999
3	2.44	0.0719	1.04	0.946	0.1739	2.52	0.999
6	5.09	0.0470	1.91	0.895	0.0649	5.17	0.998
8	6.59	0.0382	1.86	0.957	0.0609	6.68	0.999
10	8.18	0.0389	2.18	0.936	0.0565	8.24	0.999
Temperature (°C) (pH 6)							
25	2.44	0.0696	1.03	0.955	0.1610	2.52	0.999
30	2.46	0.0719	1.04	0.946	0.1754	2.52	0.999
35	2.45	0.0587	1.39	0.951	0.2042	2.50	0.999
40	2.45	0.0571	1.55	0.938	0.2329	2.50	0.999

$$q_t = k_2 q_e^2 t/(1 + k_2 q_e t) \quad (4)$$

where k_2 (g/μmol min) is the rate constant of pseudo second-order adsorption and can be determined from a linearized form of this equation, represented by Eq. 5:

$$t/q_t = 1/k_2 q_e^2 + (1/q_e)t \quad (5)$$

If second-order kinetics is applicable, the plot of t/q_t versus t should show a linear relationship. There is no need to know any parameter beforehand and the equilibrium adsorption capacity (q_e) can be calculated from Eq. 5. Contrary to the other model, it predicts the behavior over the whole range of adsorption and is in agreement with an adsorption mechanism being the rate-controlling step [17, 18], which may involve interactions between [VO(tpps)] anions and chitosan.

The slopes and y-intercepts of plots of $\log(q_e - q_t)$ versus t were used to determine the pseudo first-order rate constant (k_1) and equilibrium adsorption capacity (q_e) (figure not shown). These results are shown in Table 1. A comparison of results with the correlation coefficients (R^2) is also shown in Table 1. The values of R^2 for the pseudo first-order kinetics model were low. Also, the calculated $q_{e(cal)}$ values obtained from the pseudo first-order kinetic model do not give reasonable values, which are low compared with experimental $q_{e(exp)}$ values (Table 1). These results suggest that the adsorption kinetics of [VO(tpps)] onto chitosan 7B is not a pseudo first-order process.

The slopes and y-intercepts of plots of t/q_t versus t were used to calculate the pseudo second-order rate constant (k_2) and q_e, respectively. The straight lines in plot of t/q_t versus t showed a good agreement of experimental data with the pseudo second-order kinetic model for different initial concentrations of [VO(tpps)] (Fig. 5). Similar straight-line agreements were also observed in data taken at various

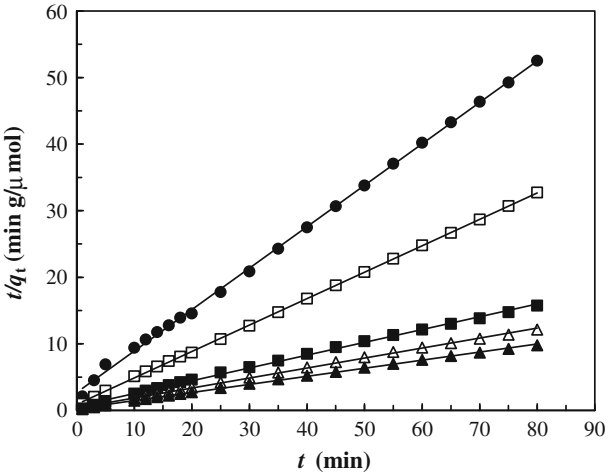

Fig. 5 Plot of the pseudo second-order model (t/q_t versus t) at different initial [VO(tpps)] concentrations (initial concentrations of [VO(tpps)]: *closed circles* 2 μmol/L, *opened squares* 3 μmol/L, *closed squares* 6 μmol/L, *opened triangles* 8 μmol/L, *closed triangles* 10 μmol/L)

pHs and temperatures although their plots are not shown in this article. The computed results obtained from the pseudo second-order kinetic model are shown in Table 1. The values of correlation coefficients (R^2) for the pseudo second-order kinetic model are ≥0.999 for all the cases. The values of calculated equilibrium adsorption capacity ($q_{e(cal)}$) also agree very well with those of experimental $q_{e(exp)}$ (Table 1) indicating a favorable condition for pseudo second-order adsorption kinetics.

Moreover, the experimental adsorption kinetic profiles (Figs. 2a, 3, and 4) are perfectly reproduced in the simulated data (each solid line in Figs. 2a, 3, and 4) obtained from numerical analysis on the basis of pseudo second-order kinetic model (Eq. 4) using the values of k_2 and $q_{e(cal)}$ listed in Table 1. These results confirm that the studied adsorption kinetics belongs to the pseudo second-order kinetic model. Similar phenomena were also observed in the adsorption of MO and RB5 onto chitosan 10B [10, 11] and biosorption of reactive dyes such as reactive blue 2 (RB2), reactive yellow 2 (RY2), and remazol black B on biomass [20, 21], respectively.

The values of k_2 at different temperatures listed in Table 1 were used to estimate the activation energy of the [VO(tpps)] adsorption onto chitosan 7B. Assume that the correlation among the rate constant (k_2), temperature (T), and activation energy (E_a) follows the Arrhenius equation, which induces the following expression:

$$\ln k_2 = -E_a/R(1/T) + \text{constant} \tag{6}$$

where R is the gas constant. The slope of plot of ln k_2 versus $1/T$ (figure not shown; correlation coefficient, $R^2 = 0.984$) was used to evaluate E_a, which was estimated to be 19.84 kJ/mol in temperature range 25–40 °C, at pH 6 and initial [VO(tpps)] concentration 3 μmol/L. Chemisorption or physisorption mechanisms are often an important indicator to describe the type of interaction between adsorbate molecule and adsorbent. The physisorption processes usually have energies in the range of 4–40 kJ/mol, while higher activation energies (40–400 kJ/mol) suggest chemisorption [22]. The value of E_a (19.84 kJ/mol) indicates that the present adsorption is a physisorption process.

To calculate the thermodynamic activation parameters such as enthalpy of activation ($\Delta H^{\ddagger}$), entropy of activation ($\Delta S^{\ddagger}$), and free energy of activation ($\Delta G^{\ddagger}$), the following relations were applied [23]:

$$\ln(k_2/T) = -\Delta H^{\ddagger}/R(1/T) + \ln(k_B/h_P) + \Delta S^{\ddagger}/R \tag{7}$$

$$\Delta G^{\ddagger} = \Delta H^{\ddagger} - T\Delta S^{\ddagger} \tag{8}$$

where k_2 (g/mol min), R, and T have the same significance as before, k_B is the Boltzmann constant ($k_B = 1.381 \times 10^{-23}$ J/K) and h_P is the Plank constant ($h_P = 6.626 \times 10^{-34}$ J s). The slope and y-intercept of the plot $\ln(k_2/T)$ versus $1/T$ (figure not shown; correlation coefficient $R^2 = 0.979$) were used to calculate $\Delta H^{\ddagger}$ and $\Delta S^{\ddagger}$, respectively. The value of $\Delta H^{\ddagger}$ was found to be 17.30 kJ/mol, which is consistent with endothermic nature of the diffusion process [23]. The value of $\Delta S^{\ddagger}$ was estimated to be −87.37 J/mol K, which reflects that no significant change occurs in the internal structure of the adsorbent material during adsorption [23, 24].

The negative $\Delta S^{\ddagger}$ values are not uncommon in adsorption, and Gupta et al. [25] and Mohan and Singh [26] have also reported negative $\Delta S^{\ddagger}$ values. The values of $\Delta G^{\ddagger}$ were estimated to be 43.34, 43.78, 44.21, and 44.65 kJ/mol at 25, 30, 35, and 40 °C, respectively. The positive values of $\Delta G^{\ddagger}$ indicate the presence of an energy barrier in the adsorption process. This is quite common and reasonable because the activated complex in the transition state is an excited form.

Equilibrium adsorption

The adsorption isotherm indicates how the [VO(tpps)] molecules distribute between the liquid phase and the solid phase when the adsorption process reaches an equilibrium state. To optimize a reaction system for the adsorption of polymers, it is important to establish the most appropriate correlation for the equilibrium curves. A plot of the equilibrium adsorption capacity, q_e (μmol/g), versus the liquid phase [VO(tpps)] equilibrium concentration, C_e (μmol/L), for various temperatures at pH 6 is shown in Fig. 6. The adsorption capacities of the chitosan increased when the solution temperature was increased from 25 to 40 °C. Various isotherm equations such as Ferundlich, Tempkin, and Langmuir were used to describe the equilibrium characteristic of adsorption. The isotherm constants were obtained from the linearized plots of respective isotherm equations and the values of correlation coefficients (R^2) are discussed in the following sections.

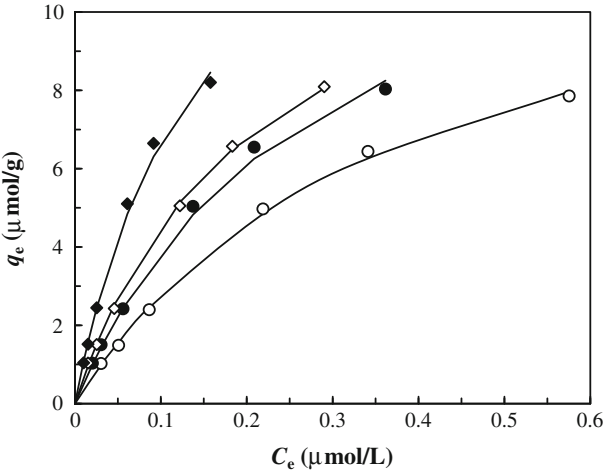

Fig. 6 Equilibrium adsorption isotherms of [VO(tpps)] onto chitosan 7B in aqueous solution at different temperatures (initial concentration of [VO(tpps)]: 1–10 μmol/L, solution volume 25 mL, chitosan 0.03 g, solution pH 6.0, temperatures: *opened circles* 25 °C, *closed circles* 30 °C, *opened squares* 35 °C, *closed squares* 40 °C). All *solid lines* are simulated equilibrium adsorption isotherms at respective temperature. The simulated equilibrium isotherms were generated using the Langmuir model in Eq. 14 and the Langmuir isotherm constants listed in Table 2

Freundlich isotherm

The well-known Freundlich isotherm [27] is based on sorption to heterogeneous surface or surfaces supporting sites of varied affinities. It is assumed that the stronger binding sites are occupied first and that the binding strength decreases with increasing degree of site occupation. The Freundlich equation is given as:

$$q_e = K_F C_e^{1/n} \tag{9}$$

The Eq. 9 can be linearized by taking logarithms to find out the parameters K_F and $1/n$.

$$\ln q_e = (1/n) \ln C_e + \ln K_F \tag{10}$$

where K_F is roughly an indicator of the adsorption capacity $((\mu mol/g)(\mu mol/L)^{-1/n})$ and n is related to the intensity of adsorption. K_F and n can be determined from the linear plot of ln q_e versus ln C_e (figure not shown). The calculated results are listed in Table 2. The magnitude of the exponent n gives an indication of the favorability

Table 2 Freundlich, Tempkin, and Langmuir isotherm constants at different temperatures and thermodynamic parameters for the adsorption of [VO(tpps)] onto chitosan from aqueous solution at pH 6

	Parameters			
Freundlich isotherm				
Temperature (°C)	25	30	35	40
K_F ((μmol/g) (μmol/L)$^{-1/n}$)	13.27	23.67	21.39	39.96
n	1.37	1.26	1.39	1.29
R^2	0.989	0.998	0.996	0.986
Tempkin isotherm				
Temperature (°C)	25	30	35	40
K_T (μmol/L)	39.22	60.40	77.04	118.92
b (J/mol)	1020.38	985.20	1013.12	913.36
R^2	0.978	0.979	0.969	0.982
Langmuir isotherm				
Temperature (°C)	25	30	35	40
K_L (L/g)	34.84	55.25	67.57	113.63
a_L (L/μmol)	2.6341	3.9779	4.9459	7.1023
a_L (L/mol)	2,634,146	2,977,901	4,945,946	7,102,273
q_m (μmol/g)	13.23	13.89	13.66	16.00
R^2	0.993	0.992	0.999	0.979
	Thermodynamic parameters			
Temperature (°C)	25	30	35	40
ΔG (kJ/mol)	−36.63	−38.28	−39.47	−41.05
ΔH (kJ/mol)	49.55			
ΔS (J/mol K)	289.38			
R^2	0.989			

of adsorption. From Table 2, the exponent n is larger than 1 for the adsorption of [VO(tpps)] by chitosan 7B at all temperatures indicating favorable adsorption under the experimental conditions [28]. However, the low values of correlation coefficients ($R^2 < 0.998$) show poor agreement of Freundlich isotherm with the experimental data.

Tempkin isotherm

The adsorption equilibrium data were analyzed by another equation, which was proposed by Tempkin and Pyzhev [29]. Tempkin isotherm contains a factor that explicitly takes into account binding species-solute interactions. This isotherm assumes that: (i) the heat of adsorption of all the molecules in the layer decreases linearly with coverage due to polymer-solute interactions, and (ii) adsorption is characterized by a uniform distribution of binding energies [29, 30]. Tempkin isotherm is represented by the following equation:

$$q_e = (RT/b)\ln(K_T C_e) \tag{11}$$

Equation 12 can be expressed in its linear form as

$$q_e = B_1 \ln K_T + B_1 \ln C_e \tag{12}$$

where

$$B_1 = RT/b \tag{13}$$

K_T (μmol/L) is the Tempkin isotherm constant, b (J/mol) is a constant related to heat of sorption, R is the gas constant (8.314 J/mol K), and T is the absolute temperature (K).

A plot of q_e versus ln C_e enables the determination of the isotherm constants b and K_T from the slope and intercept, respectively (figure not given). The calculated parameters and correlation coefficients are listed in Table 2. The Tempkin isotherm constant and the heat of adsorption changed linearly with coverage due to adsorbent–adsorbate interaction. The correlation coefficients (R^2) of the Tempkin isotherm are 0.978, 0.979, 0.969, and 0.982 at 25, 30, 35, and 40 °C, respectively. The poor correlation coefficient values showed that the experimental data was not in good agreement with the Tempkin model.

Langmuir isotherm

The widely used Langmuir isotherm [31] has found successful application in many real sorption processes and is expressed as:

$$q_e = K_L C_e/(1 + a_L C_e) \tag{14}$$

The constants K_L (L/g) and a_L (L/μmol) are the characteristics of the Langmuir equation and can be determined from a linearized form of this equation, represented by Eq. 15:

$$C_e/q_e = 1/K_L + (a_L/K_L)C_e \tag{15}$$

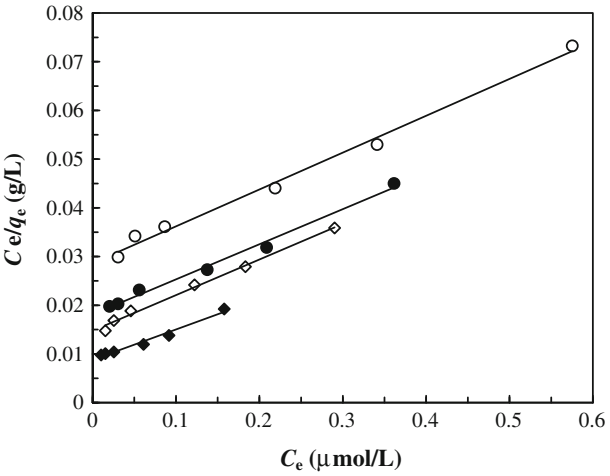

Fig. 7 Plot of Langmuir model (C_e/q_e vs. C_e) at different temperatures (*opened circles* 25 °C, *closed circles* 30 °C, *opened squares* 35 °C, *closed squares* 40 °C)

Therefore, a plot of C_e/q_e versus C_e gives a straight line of slope a_L/K_L and y-intercept $1/K_L$. The constant a_L is the Langmuir equilibrium constant and the ratio a_L/K_L gives the inverse of theoretical monolayer saturation capacity, q_m (μmol/g).

The values of K_L and a_L were computed from the slopes and y-intercepts of different linearized plots of (C_e/q_e) versus C_e representing at different temperatures (Fig. 7). The calculated results are shown in Table 2. The fits are quite well for all the four different temperatures under the concentration range studied (correlation coefficient, $R^2 \geq 0.998$). From the results shown in Table 2, the adsorption capacity of the chitosan for [VO(tpps)] is dependent on the solution temperatures. The values of a_L increased when the solution temperature was increased from about 25 to 40 °C. These results also suggest that the chitosan–[VO(tpps)] interaction must be an endothermic process.

The essential characteristics of the Langmuir isotherm can be expressed in terms of dimensionless constant separation factor (R_L) [32], which is defined as Eq. 16:

$$R_L = 1/(1 + a_L C_0) \tag{16}$$

where a_L is the Langmuir equilibrium constant and C_0 is the highest initial [VO(tpps)] concentration (μmol/L). According to the value of R_L the isotherm shape may be interpreted as described in Table 3. The values of R_L were calculated to be

Table 3 The relation between the value of R_L and type of adsorption

Value of R_L	Type of adsorption
$pR_L > 1.0$	Unfavorable
$R_L = 1.0$	Linear
$0 < R_L < 1.0$	Favorable
$R_L = 0$	Irreversible

in range between 0 and 1 at 25, 30, 35, and 40 °C, respectively, which indicates that the adsorption is favorable at all temperatures.

Moreover, in an effort to understand the equilibrium processes involved in [VO(tpps)] adsorption onto chitosan 7B, a computer simulation of the adsorption isotherms (all solid lines) has been performed numerically on the basis of the Langmuir model in Eq. 14 and using the Langmuir isotherm constants listed in Table 2, and the results are compared with the experimental data (Fig. 6). The adsorption capacities of the chitosan increased when the solution temperature was increased from 25 to 40 °C. These features of the observed data are well reproduced in the simulated data as shown in Fig. 6, supporting that the all isotherms data are described well by the Langmuir equation.

Furthermore, the thermodynamic parameters such as the changes in free energy (ΔG), enthalpy (ΔH), and entropy (ΔS) for equilibrium adsorption have been estimated to evaluate the feasibility of the adsorption process. The thermodynamic parameters were determined by using the following equations [11]:

$$\Delta G = -RT \ln a_{\mathrm{L}} \tag{17}$$

$$\ln a_{\mathrm{L}} = \Delta S/R - \Delta H/RT \tag{18}$$

where a_{L} is the equilibrium constant (L/mol) in Table 2, T is the solution temperature (K), and R is the gas constant (8.314 J/mol K). The values of ΔH and ΔS were calculated from the slope and y-intercept of van't Hoff plot of ln a_{L} vs. $1/T$ (figure not given; correlation coefficient, $R^2 = 0.989$). The results are presented in Table 2. The negative values of ΔG show that the sorption of [VO(tpps)] onto chitosan 7B was spontaneous under the experimental conditions, without requiring an induction period. An increasing trend in the negative ΔG values revealed an increasing trend in the degree of spontaneity. The values of changes in enthalpy (ΔH) and entropy (ΔS) were found to be 49.55 kJ/mol and 289.38 J/mol K ($R^2 = 0.989$), respectively. The positive value of ΔH of sorption reflects its endothermic nature, which corresponds to the results of two processes: (a) desorption of the water molecules previously adsorbed on the [VO(tpps)] and (b) adsorption of [VO(tpps)] molecules on the adsorbent. Each [VO(tpps)] molecule has to displace more than one molecule of solvent. The net result corresponds to the endothermic process. Similar results were observed in the adsorption of remacryl red TGL onto chitosan derivatives [33]. The positive value of ΔS confirms that the adsorption of the [VO(tpps)] is a combination of the two aforementioned simple processes. However, another possible interpretation of the positive changes in enthalpy and entropy could be the release of numerous water molecules from the adsorbent: the adsorption of hydrated anions onto a hydrophilic polymer network inevitably disturbs the order of water molecules in the closest environment and releases them to the external liquid. Therefore, adsorbed molecules are probably attracted because of long-distance electrostatic interactions between oppositely charge groups. During the formation of ionic bonds, counter ions should gain a higher degree of freedom and increase the entropy. The sorption of the [VO(tpps)] increasing as the temperature increases may also suggest that the number of active surface centers available for sorption increases with temperature. Furthermore, the increase in the uptake (q_{m}) of [VO(tpps)] with

temperature (Table 2) could also be a result of the enhanced rate of intraparticle diffusion of sorbate because the diffusion is an endothermic process [33]. In general, the attraction between adsorbate and adsorbent arises from van der Waals forces, hydrophobicity, hydrogen bonds, ligand exchange, dipole–dipole interactions, and chemical bonds [34]. The energy released by different forces during adsorption is unequal and the energy associated with the physical and chemical forces are van der Waals forces (4–10 kJ/mol), hydrophobic bond forces (5 kJ/mol), hydrogen bond forces (2–40 kJ/mol), coordination exchange (40 kJ/mol), dipole bond forces (2–29 kJ/mol), and chemical bond forces (>60 kJ/mol). In this study, the value of ΔH also suggests that the all above-mentioned forces were involved for adsorption of [VO(tpps)] onto chitosan 7B except chemical bond forces which is also supported by the small values of E_a (19.84 kJ/mol) and $\Delta H^{\ddagger}$ (16.96 kJ/mol) for the above adsorption process.

Conclusions

The adsorption kinetics and equilibrium adsorption of [VO(tpps)] onto chitosan 7B were studied in the present work. Batch experiments showed that the initial concentration of [VO(tpps)] significantly affects the adsorption capacity of chitosan. However, the adsorption kinetics of chitosan–[VO(tpps)] interaction is slightly influenced by the temperature. The pseudo second-order kinetic model agrees very well with the dynamical behavior for the adsorption of [VO(tpps)] onto chitosan 7B flakes under different pHs, initial [VO(tpps)] concentrations and temperatures in the whole ranges we studied. The $q_{e(cal)}$ values calculated from this kinetic model are very similar to the experimental $q_{e(exp)}$ values obtained from several experiments as shown in Table 1. The experimental adsorption kinetic profiles are well reproduced by the simulated data obtained from numerically on the basis of the pseudo second-order kinetic model in Eq. 4 and using the values of rate constants (k_2) and $q_{e(cal)}$ listed in Table 1. On the contrary, the pseudo first-order kinetic model fits the experimental data poorly for the entire range under study. Freundlich, Tempkin, and Langmuir isotherm equations were used to describe the adsorption of [VO(tpps)] onto chitosan 7B. The Langmuir equation showed the best correlation coefficient among the three models at all temperatures studied. The experimental adsorption isotherms are also well reproduced by the simulated data obtained from numerical analysis on the basis of the Langmuir model in Eq. 14 and using the Langmuir isotherm constants listed in Table 2.

The negative ΔG values show that the sorption of [VO(tpps)] onto chitosan 7B is spontaneous under experimental conditions, whereas the positive value of the enthalpy change indicates that the sorption process is endothermic in nature and the physical forces are involved in the adsorption of [VO(tpps)]. Positive value of the entropy change suggests the increase in [VO(tpps)] concentration at solid–liquid interface indicating thereby the increase in the adsorption of [VO(tpps)] onto the solid phase. It also confirms the increase in randomness at the solid–liquid interface during adsorption. The ensemble of these results clearly suggests that the readily

available chitosan 7B may be used as a potential carrier for the preparation of chitosan–[VO(tpps)] complex in aqueous solution.

Acknowledgments We are indebted to the Ministry of Science and Information & Communication Technology, Government of the People's Republic of Bangladesh for giving a special research grant (FY 2009-2010) to T. K. Saha. We are grateful to Prof. Yoshinobu Fukumori and Dr. Hideki Ichikawa (Kobe Gakuin University, Kobe, Japan) for providing the sample of chitosan 7B and measuring its particle size.

References

1. Ngaha WSW, Teonga LC, Hanafiaha MAKM (2011) Adsorption of dyes and heavy metal ions by chitosan composites: a review. Carbohydr Polym 83:1336–1456
2. Karmaker S, Saha TK, Yoshikawa Y, Sakurai H (2009) A zinc(II)-poly(γ-glutamic acid) complex as an oral therapeutic for the treatment of type 2 diabetic KKA^y mice. Macromol Biosci 9:279–286
3. Nomura CT, Taguchi S (2007) PHA synthase engineering toward superbiocatalysts for custom-made biopolymers. Appl Microbiol Biotechnol 73:969–979
4. Wu FC, Tseng RL, Juang RS (2010) A review and experimental verification of using chitosan and its derivatives as adsorbents for selected heavy metals. J Environ Manag 91:798–806
5. Yoshida H, Okamoto A, Kataoka T (1993) Adsorption of acid dye on cross-linked chitosan fibers. Chem Eng Sci 48:2267–2272
6. Kumar MNVR (2000) A review of chitin and chitosan applications. React Funct Polym 46:1–27
7. Chiou M-S, Li H-Y (2002) Equilibrium and kinetic modeling of adsorption of reactive dye on cross-linked chitosan beads. J Hazard Mater 93:233–248
8. Saha TK, Karmaker S, Ichikawa H, Fukumori Y (2005) Mechanisms and kinetics of trisodium 2-hydroxy-1,1′-azonaphthalene-3,4′,6-trisulfonate adsorption onto chitosan. J Colloid Interface Sci 286:433–439
9. Hasan M, Ahmad AL, Hameed BH (2008) Adsorption of reactive dye onto cross-linked chitosan/oil palm ash composite beads. Chem Eng J 136:164–172
10. Saha TK, Bhoumik NC, Karmaker S, Ahmed MG, Ichikawa H, Fukumori Y (2010) Adsorption of methyl orange onto chitosan from aqueous solution. J Water Resour Prot 2:898–906
11. Saha TK, Bhoumik NC, Karmaker S, Ahmed MG, Ichikawa H, Fukumori Y (2011) Adsorption characteristics of reactive black 5 from aqueous solution onto chitosan. Clean Soil Air Water 39:984–993
12. Tokumitsu H, Ichikawa H, Saha TK, Fukumori Y, Block LH (2000) Design and preparation of gadolinium-loaded chitosan particles for cancer neutron capture therapy. STP Pharma Sci 10:39–49
13. Aksungur P, Sungur A, Unal S, Iskit AB, Squier AC, Senel S (2004) Chitosan delivery systems for the treatment of oral mucositis: in vitro and in vivo studies. J Control Release 98:269–279
14. Assaad E, Wang YJ, Zhu XX, Mateescu MA (2011) Polyelectrolyte complex of carboxymethyl starch and chitosan as drug carrier for oral administration. Carbohydr Polym 84:1399–1407
15. Saha TK, Yoshikawa Y, Yasui H, Sakurai H (2006) Oxovanadium(IV)–porphyrin complex as a potent insulin-mimetic: treatment of experimental type 1 diabetic mice by [meso-tetrakis(4-sulfonatophenyl)porphyrinato]oxovanadate(IV)(4–) complex. Bull Chem Soc Jpn 79:1191–1200
16. Saha TK, Yoshikawa Y, Sakurai H (2007) Improvement in hyperglycemia and metabolic syndromes by oral treatment with the insulin-mimetic oxovanadium(IV)–porphyrin complex [meso-tetrakis (4-sulfonatophenyl)porphyrinato]oxovanadium(IV)(4–) in type 2 diabetic KKA^y mice. J Pharm Pharmacol 59:437–444
17. Lagergren S (1898) Zur theorie der sogenannten adsorption gelöster stoffe. K Sven Vetenskapsakad Handlingar 24:1–39
18. Ho YS, McKay G (1999) The sorption of lead(II) ions on peat. Water Res 33:578–584
19. Ho YS, McKay G (1999) Pseudo-second order model for sorption processes. Process Biochem 34:451–465
20. Aksu Z, Tezer S (2000) Equilibrium and kinetic modelling of biosorption of Remazol Black B by *Rhizopus arrhizus* in a batch system: effect of temperature. Process Biochem 36:431–439
21. Aksu Z (2001) Biosorption of reactive dyes by dried activated sludge: equilibrium and kinetic modeling. Biochem Eng J 7:79–84

22. Nollet H, Roels M, Lutgen P, Van der Meeren P, Verstraete W (2003) Removal of PCBs from wastewater using fly ash. Chemosphere 53:655–665
23. Petrolekas PD, Maggenakis G (2007) Kinetic studies of the liquid-phase adsorption of a reactive dye onto activated lignite. Ind Eng Chem Res 46:1326–1332
24. Singh KP, Mohan D, Sinha S, Tondon GS, Gosh D (2003) Color removal from wastewater using low-cost activated carbon derived from agricultural waste material. Ind Eng Chem Res 42:1965–1976
25. Gupta VK, Srivastava SK, Mohan D (1997) Equilibrium uptake, sorption dynamics, process optimization and column operation for the removal and recovery of malachine green from wastewater using activated carbon and activated slag. Ind Eng Chem Res 36:2207–2218
26. Mohan D, Singh KP (2002) Single and multicomponent adsorption of cadmium and zinc using activated carbon derived from bagasse—an agricultural waste. Water Res 36:2304–2318
27. Freundlich H (1906) Adsorption solution. Z Phys Chem 57:384–470
28. McKay G, Blair HS, Gardner JR (1982) Adsorption of dyes on chitin. I. Equilibrium studies. J Appl Polym Sci 27:3043–3057
29. Temkin MI, Pyzhev V (1940) Kinetics of ammonia synthesis on promoted iron catalyst. Acta Physiochim URSS 12:327–356
30. Kim Y, Kim C, Choi I, Rengraj S, Yi J (2004) Arsenic removal using mesoporous alumina prepared via a templating method. Environ Sci Technol 38:924–931
31. Langmuir I (1918) Adsorption of gases on plane surfaces of glass, mica platinum. J Am Chem Soc 40:1361–1403
32. Hall KR, Eagleton LC, Acrivers A, Vermenlem T (1966) Pore- and solid-diffusion kinetics in fixed-bed adsorption under constant-pattern conditions. Ind Eng Chem Fundam 5:212–223
33. Lazaridis NK, Kyzas GZ, Vassiliou AA, Bikiaris DN (2007) Chitosan derivatives as biosobents for basic dyes. Langmuir 23:7634–7643
34. Ahmad R, Kumar R (2011) Adsorption of amaranth dye onto alumina reinforced polystyrene. Clean Soil Air Water 39:74–82